A Permanent Magnet Synchronous Generator Control Approach for Stand-alone Gas Engine Generation System

Htar Su Hlaing, Yushi Miura, Toshifumi Ise
Division of Electrical, Electronics and Information Engineering
Graduate School of Engineering, Osaka University
2-1 Yamadaoka, Suita, Osaka, Japan

***Abstract*—This paper addresses a control strategy for permanent magnet synchronous generator (PMSG) interconnected to the load through a back-to-back converter for stand-alone gas engine generation system. The engine generator system with a diode rectifier causes harmonic currents in the generator which can affect generator efficiency and produce torque oscillations. Using an insulated gate bipolar transistor (IGBT) rectifier instead of the diode rectifier enables us to improve current waveforms and to control output voltage of PMSG. In the proposed control scheme, the generator side converter is controlled by means of a vector control method which is based on the mathematical model of PMSG and rectifier in the stator-oriented dq-reference frame. Using this control strategy, we obtain a controllable dc-link voltage and can control generator stator voltage to its rated value. For load side inverter control, the concept of virtual synchronous generator (VSG) control is adopted to support smooth transients between islanding and grid connected operation. Simulation is carried out to analyze system responses under loading and unloading conditions. The simulation results show usefulness of the proposed control structure.**

Keywords—PMSG, back-to-back converter,vector control,VSG

I. INTRODUCTION

Gas engine generators can provide electrical power in places where utility power is not available or in emergency case where power is temporarily needed. The important advantage is that they can operate in parallel with the local grid, or can be used in isolated sites. There are many different kinds of generators that can be used in engine generation system. Recently, permanent magnet synchronous generator becomes popular for its higher efficiency, no excitation losses, smaller size, and less weight in comparison to other types of generators [1]-[2].

In the engine power generation system, generated power is delivered to the load or grid by using a power electronic unit which performs power conversion process. In practice, two schemes of power conversion are used for ac to dc power conversion process. The first one is based on an uncontrolled diode rectifier which is easy and simple to implement. In the second one, the Insulated Gate Bipolar Transistors (IGBTs) based rectifier which is controlled by the pulse width modulation (PWM) method is applied. In both cases, the voltage source inverter is coupled with the power grid or load by using transformer or inductive choke. The first method of energy conversion can cause harmonic distortion of the generator currents. The major disadvantages of these harmonic currents are overheating because of increased losses and mechanical oscillations due to the pulsating torque. As a consequence, the generator efficiency will be significantly affected. These harmonic distortions can be reduced by the second method. An application of IGBT rectifier results in nearly sinusoidal waveform of the generator currents, so it enables us to reduce the additional losses of the generator.

In this research, the second method is adopted for stand-alone engine generation system as shown in Fig. 1. The overall system consists of an engine, a PMSG, two IGBT-based power converters connected in back-to-back via a dc-link and a load. In addition, the control algorithms for two power converters are also included. The main functions of the generator side converter are to stabilize dc-link voltage and to control generator stator voltage by means of vector control approach. The load side converter which is controlled by virtual synchronous generator (VSG) supports smooth transients between islanding and grid connected operation. The mathematical model of PMSG is presented in section Ⅱ. The main circuit and individual parts of the proposed control structure are explained in section Ⅲ. The simulation results are discussed in section Ⅳ. Finally, the paper is concluded in section Ⅴ.

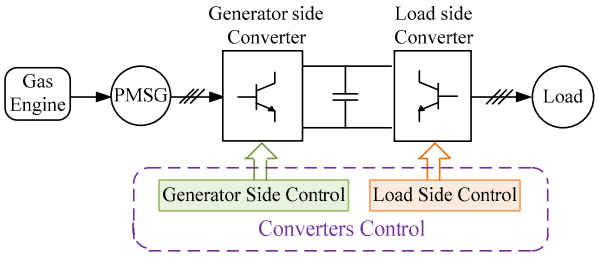

Fig. 1 Topology of a gas engine generation system

978-1-5090-1210-7/16/$31.00 ©2016 IEEE

II. PERMANENT MAGNET SYNCHRONOUS GENERATOR

The per-phase equivalent circuit and phasor diagram of PMSG are shown in Fig.2. In Fig.2 (a), R_s is stator resistance, L_s is stator inductance, I_s is stator current, ω_r is rotor speed of generator and U_s is stator voltage. The back electromotive force (E) induced in the stator by permanent magnet flux (ψ_{PM}) can be expressed as

$$E = j\omega_r \psi_{PM} \tag{1}$$

Thus, the induced voltage E depends on the actual rotor speed of generator. The induced voltage and the stator voltage are equal for no-load condition. However, as can be seen in Fig. 2(b), the voltage drop due to the machine's reactance causes a phase delay (the load angle δ) between the induced voltage and the stator voltage under load condition. Thus, the stator voltage is smaller than the induced voltage under load condition.

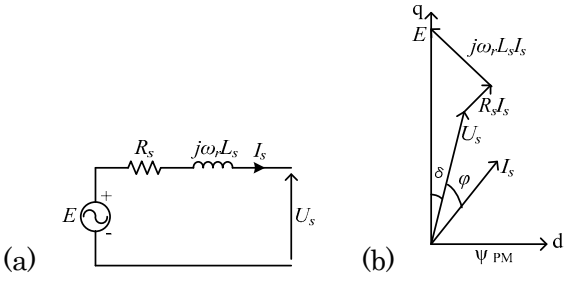

Fig. 2 (a) Per-phase equivalent circuit, (b) phasor diagram of PMSG

By using a standard dq-coordination system, the stator voltage equations of PMSG in the rotor reference frame can be written as

$$u_{ds} = -R_s i_{ds} + \omega_r L_q i_{qs} \tag{2}$$

$$u_{qs} = -R_s i_{qs} - \omega_r L_d i_{ds} + \psi_{PM} \tag{3}$$

Here, u_{ds} and u_{qs} are the generator terminal stator voltages, i_{ds} and i_{qs} are the stator currents, L_d and L_q are the stator inductances in the dq-reference frame.

If the PMSG is assumed to be a surface mounted type, electromagnetic torque can be expressed as

$$T_e = \psi_{PM} i_{qs} \tag{4}$$

In the stator voltage-oriented reference frame, the stator voltage is aligned in the d-axis and the stator voltage on q-axis is equal to zero. Then, the active power and reactive power of the PMSG are given by

$$P_s = u_{ds} i_{ds} \tag{5}$$

$$Q_s = -u_{ds} i_{qs} \tag{6}$$

Again, the relationship between ac input power and dc output power of the rectifier can be written as

$$P_s = u_{ds} i_{ds} = P_{dc} = v_{dc} i_{dc} \tag{7}$$

Based on the above concepts and explanations, we can see that the active power depends on the stator current d-components, while the reactive power depends on the stator current q-components. Hence, the dc side voltage v_{dc} is proportional to the stator current d-component i_{ds} so that the dc side voltage of rectifier can be controlled by the control of i_{ds}. Since the generated active power is fed via the dc-link to the load, it is necessary to control the dc-link voltage in order to maintain reference value. On the other hand, the stator voltage U_s can be controlled by the control of the stator current q-component i_{qs}. In the PMSG system, the stator voltage is decreased under load condition because of no excitation control. Moreover, the stator voltage varies depending on the generator speed. This can cause over-voltages for the converter and the generator in case of over-speeds. In order to overcome these problems, the stator voltage is controlled in its rated value by controlling the stator current q-component i_{qs}.

III. MAIN CIRCUIT AND CONTROL STRUCTURE

Figure 3 shows the main circuit structure of the engine generation system studied in this paper. As illustrated in the figure, the gas engine is directly connected to the PMSG. The gas engine model is represented by a speed control loop and provides a controlled torque (T_m) to the PMSG. The PMSG produces uncontrolled 3-phase voltages (u_a, u_b, u_c) and currents (i_a, i_b, i_c) which are the inputs to the generator side converter (GSC). The GSC outputs the demanded dc-link voltage (V_{dc}) by means of PWM. Then, the load side converter (LSC) converts the dc-link voltage to the ac grid voltage with the fixed system frequency of the load side. The filters (L_{fm}, L_{fL} and C_{fL}) are connected to each ac side of the converter in order to reduce voltage and current ripples caused by each converter. The circuit parameters of the main circuit and PMSG are listed in Tables Ⅰ and Ⅱ, respectively.

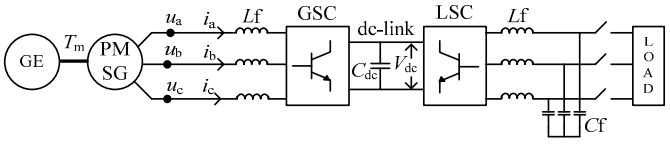

Fig. 3 Main circuit configuration

TABLE I. CIRCUIT PARAMETERS

L_{fm}	2 mH	L_{fL}	1 mH
C_{dc}	30mF	C_{fL}	10 μF
V_{dc}*	400 V	ω*	1710 rpm

TABLE II. PARAMETERS OF PMSG

Output power	10 kW	Rated voltage, U_s*	210 V
R_a	0.0051716 pu	Per unit inertia constant	0.08 s
X_d	0.219 pu	X_q	0.219 pu
X_d'	0.027 pu	X_q'	0.027 pu
X_d"	0.01 pu	X_q"	0.01 pu
T_{d0}'	6.55 s	T_{q0}'	0.85 s
T_{d0}"	0.039 s	T_{q0}"	0.071 s

Using a back-to- back converter allows full controllability of the system. In this paper, the power converter control structure can be described by two parts: a controller for generator side converter and a controller for load side converter. Therefore, the overall control structure consists of three control schemes and they are explained in the following subsections.

A. Gas engine speed controller

The gas engine speed controller uses the engine speed or generator frequency as control input. The following block diagram in Fig.4 represents the speed control loop of gas engine. ω_G* is the reference speed. ω_G is the actual speed of engine. The error between the reference speed and measured speed is sent to the Proportional and Integral (PI) controller. The output of PI controller is the input mechanical torque to the generator. In this study, the value of proportional gain K_{pG} is 0.035 and the value of integral time constant T_G is 1.0 s.

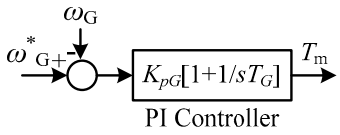

Fig. 4 Block diagram of gas engine speed controller

B. Generator side converter control

The generator side converter performs the function of DC voltage regulation as well as stator voltage control of the generator by means of vector control method. According to the applied vector control, the generator stator voltages and currents are transformed to the rotating dq co-ordination system, and are used as feedback variables for the performed controller as shown in Fig. 5. The voltage angle for dq-transformation is extracted from a phase-locked loop (PLL) circuit. This circuit is implemented in synchronous dq reference frame. The phase-locking of the system is done by adjusting the q-axis voltage to zero. A PI controller is used for this purpose. By integrating the sum of the PI output and the reference frequency f_0, the voltage angle is obtained. This angle is used for all dq transformations of GSC control scheme.

The controller for GSC is a cascaded control structure with an inner current controller and an outer voltage controller. It consists of four PI controllers, decoupling factors and feed-forward terms. The control structure is organized as shown in Fig. 5. Thus, PI 1 in Fig. 5 is a dc-link voltage controller which corresponds to active power. PI 2 is stator voltage control loop. These two outer controllers are employed to control the dc-link voltage and the generator stator voltage in a way that the voltages will return to their reference values after a load has been applied or rejected. PI 3 and PI 4 correspond to both d- and q-axis current controllers, respectively.

When the engine generator is operating in the stand-alone mode, the engine speed cannot response immediately to the sudden load changes and cannot provide the power drawn by the load. Meanwhile, the energy stored in the dc-link is delivered to the load under the power transient conditions. Therefore, in this study, the PI parameters are tuned to get a slow response in order to deliver the discharged energy mainly from the dc-link capacitance to the load during the sudden load changes. The transfer function of PI controller used in this paper is

$$F(s) = K_p + \frac{1}{sT} \tag{8}$$

In here, K_p is a proportional gain and T is an integral time constant. The PI parameters for all controllers are tuned by try-and-cut approach and listed in Table III.

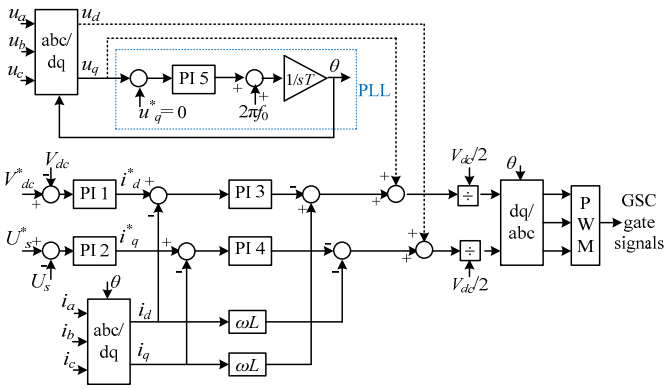

Fig. 5 Generator side converter control structure

TABLE III. PI PARAMETERS

	K_p	T
PI 1	0.3	10 s
PI 2	1	5 s
PI 3	20	0.1 s
PI 4	3	0.1 s
PI 5	50	0.05

C. Load side converter control

The VSG was proposed to control the load connected inverter as shown in Fig. 6. In this scheme, the well-known swing equation expressed in (9) is used to realize the characteristic of a typical synchronous generator.

$$P_{in} - P_{out} = J\omega_m \frac{d\omega_m}{dt} - D\Delta\omega_m \tag{9}$$

where, P_{in} and P_{out} are input and output powers; J is the inertia moment, and D is the damping factor. ω_m is the virtual angular velocity of the virtual rotor, $\Delta\omega_m$ is the virtual angular velocity deviation of the virtual rotor.

As shown in Fig. 6, the output power and grid frequency are calculated by using inverter output voltages and currents. Then, (9) can be solved by numerical integration. By solving this equation in each control cycle, the momentary frequency ω_m is calculated and by passing through an integrator, the virtual mechanical phase angle, θ_m is produced for generating

PWM pulses. The VSG has an inertia and ability to synchronize with the grid automatically, like a synchronous generator. The VSG is applied to this stand-alone system for the purpose of supporting smooth transients between islanding and grid connected operation. The parameters for VSG control scheme are shown in Table IV. The block diagram of AVR of VSG is shown in Fig. 7. The detailed structure of governor and load frequency control for VSG is presented in Fig.8.

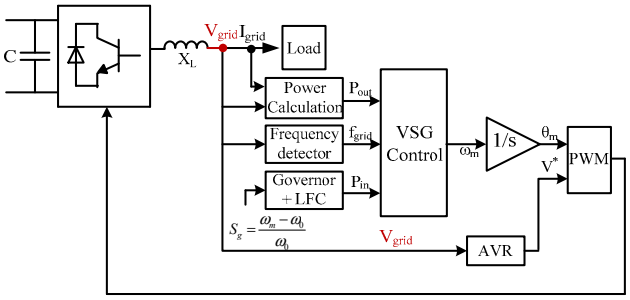

Fig. 6 Load side converter control structure

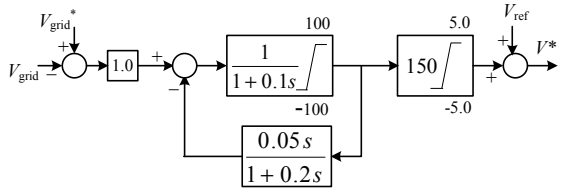

Fig. 7 AVR of VSG

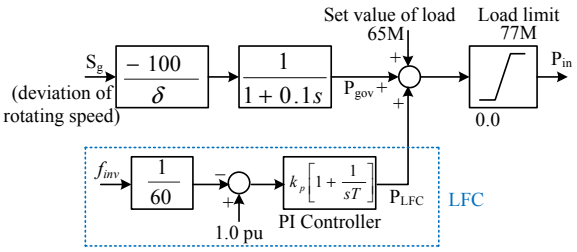

Fig. 8 Governor and load frequency control (LFC)

TABLE IV. PARAMETERS FOR VSG CONTROL

Rated Power P_{base}	10 kW	Rated voltage V	200 V
Rated Frequency f_0	60 Hz	Speed regulation factor δ	5 %
Per-unit inertia constant M	10 s	Inertia moment J	2.4627 kg.m
Damping factor D	0.0451 s/rad	Switching frequency f	15 kHz
LFC PI gain	20	LFC PI time constant	0.5 s
Output voltage command	200 V	dc-link capacitance C	30 mF

IV. SIMULATION

Some computer simulations are carried out to test the response of the proposed control scheme by PSCAD/EMTDC software. To verify the effectiveness of using an IGBT rectifier, simulations are performed for two different system topologies: system with a diode rectifier and system with an IGBT rectifier for the generator side converter. The same system parameters are used for both cases because the IGBT rectifier behaves as a diode full-bridge rectifier under the gate-blocking condition due to the diodes connected to IGBT in an anti-parallel structure. The simulations are performed for the system shown in Fig. 3. At first, simulation is carried out for the system with diode rectifier. The total simulation time is fixed at 40 s. The generator is initialized to run at speed of 1710 rpm without load. After 5 s, the full load is applied and the system response to the step load change from 0 kW to 9 kW is analyzed.

The generator speed response to the step load increase is shown in Fig. 9(a). There is a speed dip of 240 rpm due to the applied load. However, after 4 s, the speed can catch its reference value. Fig. 9(b) shows the dc-link voltage response, and it can be seen a significant voltage drop of 68 V at the start of loading. Moreover, the dc voltage is maintained around 240 V at steady state, and cannot reach to its maximum value of 298 V because there is no control for both generator field voltage and dc-link. The generator stator voltage response is shown in Fig. 9(c). The stator voltage decreases from its rated voltage of 210 V to 180 V during the load transients and operating around 190 V at steady state. There can be seen large voltage transients due to the step load change on both dc-link voltage and generated stator voltage. In Fig. 9(d), the generated power and load output power are described. As can be seen, there are high oscillations in the generated power due to distorted waveform of generator current, and a small transient in the load power. As shown in Fig. 9(e), the generator output current contains large harmonic contents that can deteriorate the generator efficiency. The inverter output voltage and current waveforms in Fig. 9(f) are disturbed waveforms because decreasing dc voltage cannot support the rated voltage of the load.

At 30 s of the simulation time, the load is removed from the system, and the system responses from 9 kW to 0 kW are obtained as shown in Fig. 10. From these results, the speed rise of 210 rpm in Fig. 10(a) is smaller than the speed dip of loading case. The dc-link voltage and the stator voltage reach to their original values after load has been removed. The generator output power and load power also change from full load to no load without any oscillation.

In the next step, simulation for the system with the IGBT rectifier is performed. Similarly, here the total simulation time is also fixed at 40 s. At first, the generator is running at speed of 1710 rpm without the load. After 5 s, the full load is applied; and the system response to the step load change (from 0 kW to 9 kW) is analyzed. Then, at time 30 s, the load is removed from the system in order to see the system response to the load change from 9 kW to 0 kW.

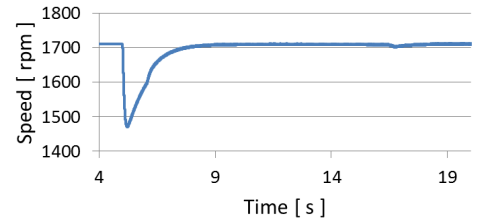

(a)

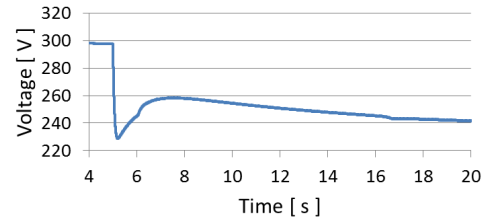

(b)

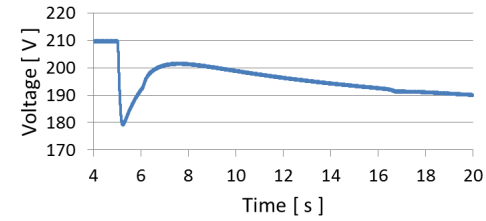

(c)

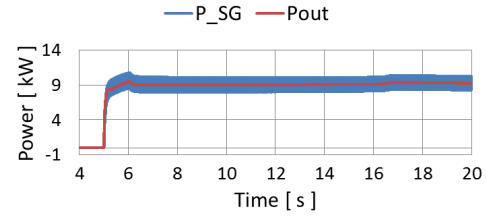

(d)

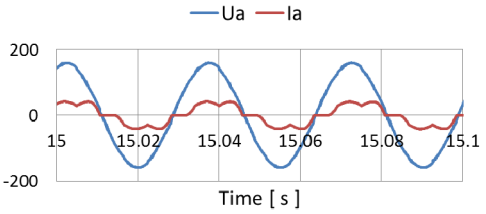

(e)

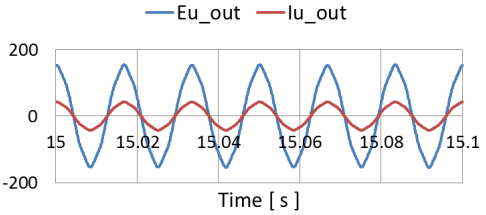

(f)

Fig. 9 Simulation results of 9 kW loading case with a diode rectifier (a) generator speed, (b) dc-link voltage, (c) stator voltage, (d) generator output power and load power, (e) generator output voltage and current in steady state [Phase a], (f) inverter output voltage and current in steady state [Phase a]

The generator speed response to the step load increase is shown in Fig. 11(a). When the load is connected to the system, there is a decrease in generator speed around 230 rpm, about 10 rpm smaller than that of the diode case. After 4 s, the speed can catch its reference value, properly. Fig. 11(b) shows the dc-link voltage response. The amount of voltage drop at the start of load connection is also significant. However, the dc voltage reaches its reference value after 13 s without overshoot and steady state error. This result shows the usefulness of dc-link voltage controller. In Fig. 11(c), the stator voltage drop is smaller than that of diode case and this voltage dip can reach at 209 V (that is very close to its rated value) which shows the usefulness of stator voltage controller. In Fig. 11(d), the generated power and load output power are indicated. Comparing with the result of diode case, the power oscillations in the generator power are significantly suppressed. The difference between the generator power and load power which represents the losses in the converters is very small.

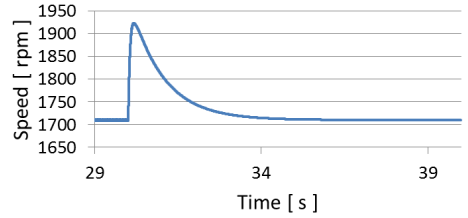

(a)

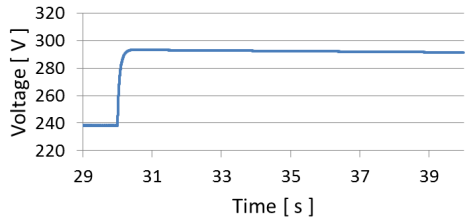

(b)

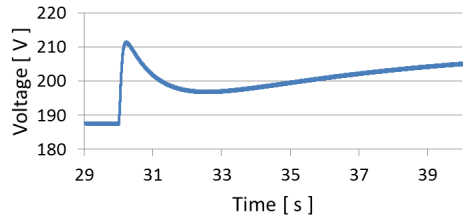

(c)

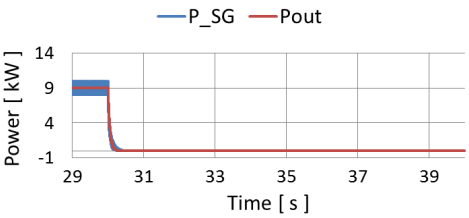

(d)

Fig. 10 Simulation results of 9 kW unloading case with a diode rectifier (a) generator speed, (b) dc-link voltage, (c) stator voltage, (d) generator output power and load power

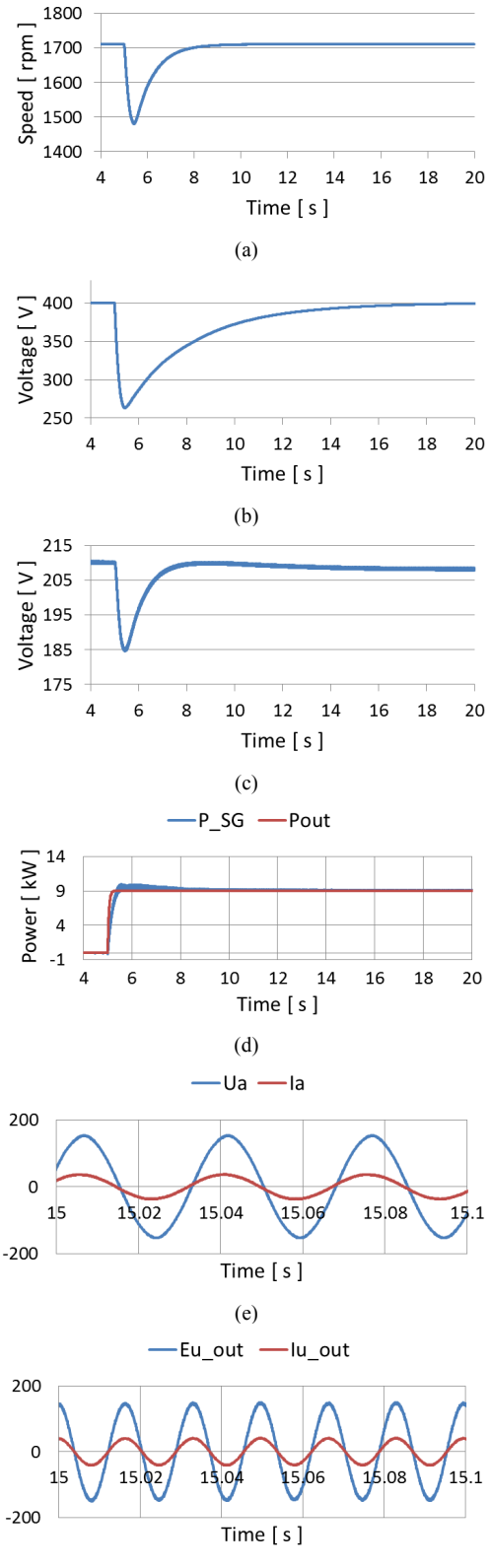

Fig. 11 Simulation results of 9 kW loading case with an IGBT rectifier (a) generator speed, (b) dc-link voltage, (c) stator voltage, (d) generator output power and load power, (e) generator output voltage and current in steady state [Phase a], (f) inverter output voltage and current in steady state [Phase a]

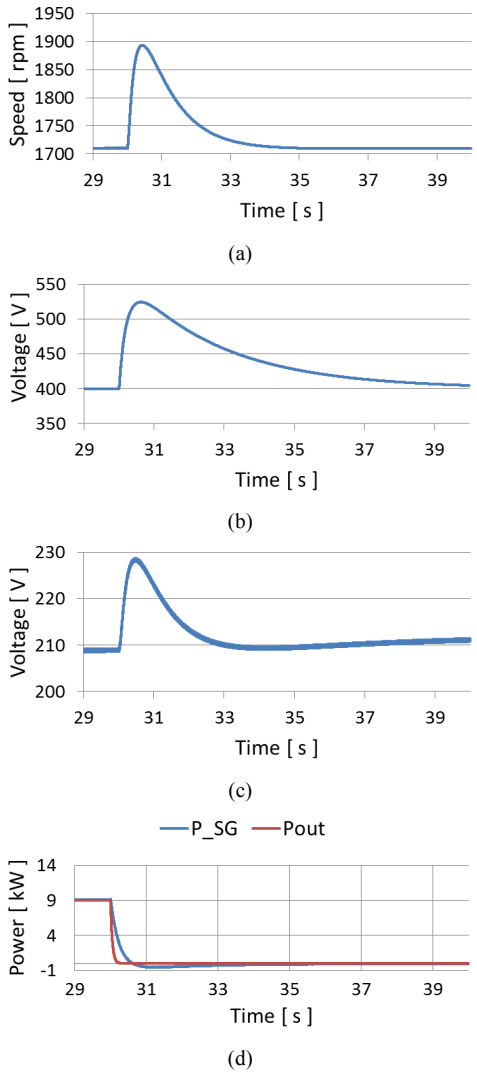

Fig. 12 Simulation results of 9 kW unloading case with an IGBT rectifier (a) generator speed, (b) dc-link voltage, (c) stator voltage, (d) generator output power and load power

Fig. 11(e) illustrates that the current is very close to the sinusoidal waveform and the harmonic contents in the generator current are greatly reduced. It can also be seen that the waveforms of inverter output voltage and current are also sinusoidal. Fig. 12 analyzes the system responses when the load is removed from the system. In this case, the speed rise, the dc voltage rise and stator voltage rise have smaller values compared to the loading case. The generator output power and load power also have a smooth change.

Compared to system with diode rectifier, the applied system configuration and control method is obviously effective for harmonic reduction in generator current by improving the current waveform. Moreover, the dc-link voltage and generator stator voltage are controlled to reach their reference values after load transients. In this system, the output of dc voltage is higher than the input ac voltage; because the IGBT rectifier is a boost type converter. Thus, it can provide the rated load without any distortion.

However, the generator speed deviation due to load changes is very significant for the above two systems. In the stand-alone gas engine system, the engine speed variation is restricted by an upper and lower limit. In order to operate the engine generator within its limits, the power balance is adjusted by the voltage drop of the dc-link capacitor under load transient conditions. The voltage drop of the dc-link capacitor, known as the discharged energy, is the energy difference between generator and load. The discharged energy from the dc-link can be represented as

$$W = \frac{1}{2}C(\Delta V^2) = \frac{1}{2}C(V_0^2 - V_f^2) \tag{10}$$

Here, W is the discharged energy from the dc-link, C is the value of capacitance at dc-link, V_0 is the initial dc voltage and V_f is the final dc voltage.

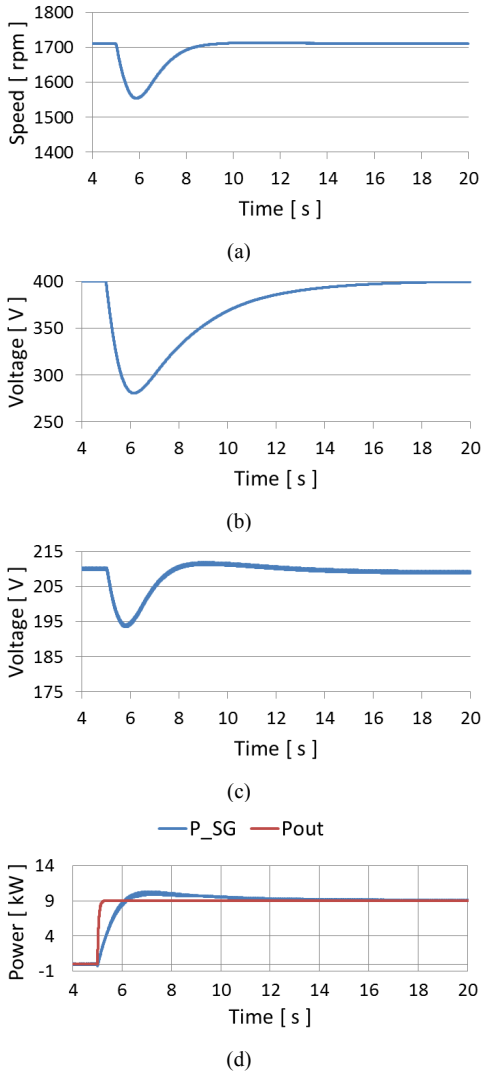

Fig. 13 Simulation results of 9 kW loading case with 100mF (a) Generator Speed, (b) dc-link voltage, (c) Stator voltage, (d) Generator output power and Load power

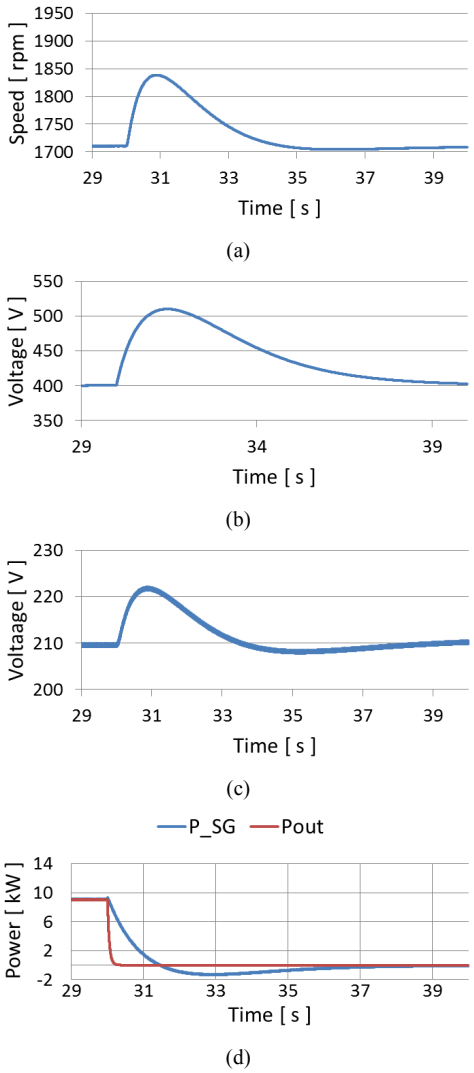

Fig. 14 Simulation results of 9 kW unloading case with 100mF (a) Generator Speed, (b) dc-link voltage, (c) Stator voltage, (d) Generator output power and Load power

For the system with the IGBT rectifier, the initial dc voltage is 400 V and the final dc voltage is 260 V as depicted in Fig. 11(b). The amount of discharged energy during the load transients is 1386 J.

In order to test the system response with large capacitance value in the dc-link, the system with the IGBT rectifier is simulated again by increasing the value of capacitance from 30 mF to 100 mF. Apart from the capacitance value, all remaining parameters are the same with the previous one. The obtained results are compared with the previous one by important characteristics. In Fig. 13(a), the speed dip is reduced to 1550 rpm. The dc-link voltage drop and stator voltage drop are also reduced compared to the results of the system with 30 mF. Fig. 13(b), the initial dc voltage is 400 V and the final dc voltage is 280 V. Using (10), the amount of discharged energy is 4080 J. Fig. 13(d) shows that the generator power builds up slowly to provide the power drawn by the load. Meanwhile, the discharged power from dc-link is

providing energy to the load. Figure 14 shows the simulation results of the system with 100 mF for unloading case. It can be said that the overall system responses can be improved if the discharge energy from the dc-link is high enough for the load transient conditions.

V. Discussion on Capacitor Value

To determine the reasonable capacitance value, the analysis can be expressed in Fig. 15. When the load power increases by ΔP_L at time $t = 0$, the generator output power ΔP_G will increase accordingly. The generator output power can reach the load power at t_r.

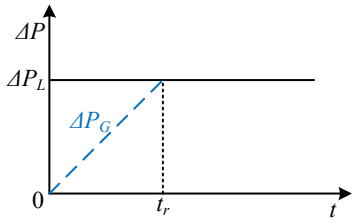

Fig. 15 Power response during step load increase

Let the slope of the ΔP_G is k, then k can be written as

$$k = \frac{\Delta P_L}{t_r} \tag{11}$$

The energy difference between generator and load can be expressed as

$$W = \frac{1}{2}\Delta P_L t_r = \frac{1}{2}\frac{\Delta P_L^2}{k} \tag{12}$$

This equation can be expressed in terms of capacitor voltage and becomes

$$\frac{1}{2}C\left(V_{dc}^2(0) - V_{dc}^2(t_r)\right) = \frac{1}{2}\frac{\Delta P_L^2}{k} \tag{13}$$

Thus, the value of capacitance can be derived as

$$C = \frac{\Delta P_L^2}{k\left(V_{dc}^2(0) - V_{dc}^2(t_r)\right)} \tag{14}$$

Hence, the capacitor value and the dc-link voltage drop affect the power response. It can be observed that the larger capacitance value and the dc-link voltage drop will cause the slower generator power response which can reduce the speed deviation of generator speed. Therefore, the selection of capacitance value plays an important role in the stand-alone system. Whether the capacitance values used in this paper are enough for the specified load power of 9 kW or not will be analyzed by the concept of power response during step load change which is illustrated in Fig. 15. This analysis will be an extended work of this paper.

VI. Conclusion

This paper mainly investigates the entire control system for gas engine generation with PMSG and back-to-back converter where an IGBT rectifier is used instead of a diode rectifier. In this study, control strategies for generator side converter and load side converter are implemented. Using the applied control structure, the active power and reactive power of the generator are controlled independently. Active power is controlled by the dc-link voltage controller while reactive power is controlled by the generator stator voltage control loop. In order to show the effectiveness of the proposed control structure, some computer simulations are done under step load change condition while the generator is operating in stand-alone mode. Compared to system with diode rectifier, the applied system configuration and control method is obviously effective for harmonic reduction in generator current by improving the current waveform. Thus, improvement of generator efficiency is expected. Moreover, the dc-link voltage controller supports the discharged power under load transient conditions to suppress the deviation of gas engine rotational speed. Therefore, the proposed control approach for PMSG is suitable for stand-alone gas engine generation system.

References

[1] Monica Chinchilla, Santiago Arnaltes and Juan Carlos Burgos : "Control of Permanent-Magnet Generators Applied to Variable-Speed Wind-Energy Systems", IEEE Transactions on Energy Conversion, Vol.21, No.1, pp.130-135 (2006)

[2] Xibo Yuan, Fei (Fred) Wang and Dushan Boroyevich: "DC-link Voltage Control of a Full Power Converter for Wind Generator Operating in Weak-Grid Systems", IEEE Transactions on Power Electronics, Vol.24, No.9, pp.2178-2192 (2009)

[3] Shuhui Li, Timothy A.Haskew and Ling Xu: "Control of HVDC Light System Using Conventional and Direct Current Vector Control", IEEE Transactions on Power Electronics, Vol.25, No.12, pp.3106-3118 (2010)

[4] Chandra Bajracharya, Marta Molinas, Jon Are Suul and Tore M Undeland: "Understanding of tuning techniques of converter controllers for VSC-HVDC", Nordic Workshop on Power and Industrial Electronics, (2008)

[5] Azziddin M.Razail and M.A. Rahman: "Virtual Grid Flux Oriented Control Method for Front-End Three Phase Boost Type Voltage Source Rectifier", 25th IEEE Canadian Conference on Electrical and Computer Engineering, (2012)

[6] Hassan Bevrani, Toshifumi Ise and Yushi Miura: "Virtual synchronous generators: A survey and new perspectives", Electrical Power and Energy Systems 54, pp. 244 – 254 (2014)

[7] Y.Banjo, Y. Miura, T. Ise and T. Shintai: "Enhanced Stand-Alone Operating Characteristics of an Engine Generator Interconnected through the Inverter using Virtual Synchronous Generator Control", 9th International Conference on Power Electronics-ECCE Asia, ICPE 2015-ECCE Asia, June 1-5, Seoul, Korea, pp.WeG1-4 (2015)

[8] Htar Su Hlaing, Yushi Miura and Toshifumi Ise: "Application of Back-to-Back Converter to an Engine Generation System using a Permanent Magnet Synchronous Generator", Technical Meeting on Power Engineering and Power System Engineering, Touhoku University, Japan, September 16-18, PE-15-069, PSE-15-091, pp. 11-16 (2015)